Effects of cladding radius on the optical characteristics of long-period fiber gratings*

DONG Xiao-wei (董小伟)**, **QUAN Wei** (权炜), **and XIE Yuan** (谢媛)
College of Information Engineering, North China University of Technology, Beijing 100144, China

(Received 12 October 2013)

Using three-layer vector field model, the dispersion characteristics and spectral response of long-period fiber gratings (LPFGs) with different cladding radii are analyzed. Both the numerical and experimental results demonstrate that LPFG's resonant wavelengths shift towards much longer wavelength and the transmission depth is strengthened significantly by decreasing cladding radius. When the cladding radius is less than 20 μm, only a single resonant peak over a wavelength range of 600 nm (from 1200 nm to 1800 nm) is achieved, and the sensitivity of LPFG to external refractive index is enhanced significantly.

Document code: A **Article ID:** 1673-1905(2014)01-0067-4
DOI 10.1007/s11801-014-3193-9

In recent years, long-period fiber grating (LPFG) has found many potential applications in optical communication[1] and optical fiber sensor[2,3]. LPFG is a photosensitive or hydrogen-loaded single-mode optical fiber with the core inscribed by axially periodic refractive index modulation. It couples light from core mode to co-propagating higher-order cladding modes which are primarily guided by fiber cladding. Therefore, the structure of fiber plays a very important role on LPFG's transmission spectrum[4]. Although there are several studies about the effect of cladding radius on LPFG's characteristics[5-7], most of them are focused on the resonant coupling between the core mode and the lower-order cladding mode under the cladding radius larger than 50 μm, and only demonstrate the wavelength shift for different cladding radii. However, the characteristics of LPFG here mean not only the resonant wavelength but also its transmission depth. Therefore, in this paper, by using three-layer vector field model, we make a complete theoretical and experimental investigation for the effects of cladding radius on both resonant wavelength and transmission depth of LPFG. And an ultra-sensitive LPFG to the surrounding refractive index is achieved by reducing the cladding radius.

Based on coupled-mode theory[8], the pth resonant wavelength λ_p of LPFG is specified by the phase-matching condition between core mode and cladding mode of fiber:

$$2\pi / \Lambda = (\beta_{\text{co}} - \beta_{\text{cl}}) = (n_{\text{effco}} - n_{\text{effcl}}) \cdot 2\pi / \lambda_p , \tag{1}$$

where Λ is the grating period, β_{co} and β_{cl} are the propagating constants of fiber's core mode and cladding mode, and n_{effco} and n_{effcl} are the effective indices of core mode and cladding mode. The corresponding transmission depth is

$$T(\lambda_p) = \cos^2(k_p L), \tag{2}$$

where k_p is the coupling coefficient, and L is the grating length.

Due to the structure dependency of the propagating constants, when the cladding radius is changed, the central resonant wavelength is tuned[9]. At the same time, both the wavelength shift and the cladding radius variation lead to the change of the coupling coefficient, which is determined by the overlap integration between core mode and cladding mode. Thus, the transmission depth can also be adjusted correspondingly. In order to make a detailed investigation about the effect of cladding radius, the precise dispersion equation describing the three-layer waveguide modeling should be derived firstly. Based on the Maxwell equation, the longitudinal field components of e_z and h_z must satisfy the Helmoholtz equation in the cylindrical coordinate system as[10]

$$\frac{\mathrm{d}^2\Psi}{\mathrm{d}r^2} + \frac{1}{r}\frac{\mathrm{d}\Psi}{\mathrm{d}r} + (k_0^2 n_i^2 - \beta^2 - \frac{m^2}{r^2})\Psi = 0 , \tag{3}$$

where complex amplitude $\Psi(r, \varphi, z)$ represents the electric or magnetic field components, $k_0=2\pi/\lambda$ is the wave vector in free space, n_i (i=1, 2, 3) is the refractive index of each layer, and m is the azimuthal order. Utilizing the relationship between transverse components and longitudinal components, the transverse field components can be obtained from longitudinal components, which can be expressed in matrix format as follows: in the fiber core,

* This work has been supported by the National Natural Science Foundation of China (No.61007007), the Talents of North China University of Technology (No.CCXZ201307), the Foundation of Beijing Municipal Committee of CPC Organization Department (No.2012D005002000001), and the Importation and Development of High-Caliber Talents Project of Beijing Municipal Institutions.
** E-mail: way7803@163.com

$$\begin{bmatrix} e_\varphi \\ h_\varphi \\ e_z \\ h_z \end{bmatrix} = \begin{bmatrix} -\dfrac{m\beta a_1^2}{U^2 r} J_m(Ur/a_1) & \dfrac{\mathrm{j}\omega u_0 a_1}{U} J'_m(Ur/a_1) \\ -\dfrac{\mathrm{j}\omega\varepsilon a_1}{U} J'_m(Ur/a_1) & -\dfrac{m\beta a_1^2}{U^2 r} J_m(Ur/a_1) \\ J_m(Ur/a_1) & 0 \\ 0 & J_m(Ur/a_1) \end{bmatrix} \cdot \begin{bmatrix} A_1 \\ C_1 \end{bmatrix} = M_1(r) \begin{bmatrix} A_1 \\ C_1 \end{bmatrix}, \quad (4)$$

and in the surrounding layer,

$$\begin{bmatrix} e_\varphi \\ h_\varphi \\ e_z \\ h_z \end{bmatrix} = \begin{bmatrix} \dfrac{m\beta a_2^2}{W^2 r} K_m(Wr/a_2) & -\dfrac{\mathrm{j}\omega u_0 a_2}{W} K'_m(Wr/a_2) \\ \dfrac{\mathrm{j}\omega\varepsilon a_2}{W} K'_m(Wr/a_2) & \dfrac{m\beta a_2^2}{W^2 r} K_m(Wr/a_2) \\ K_m(Wr/a_2) & 0 \\ 0 & K_m(Wr/a_2) \end{bmatrix} \cdot \begin{bmatrix} B_3 \\ D_3 \end{bmatrix} = M_3(r) \begin{bmatrix} B_3 \\ D_3 \end{bmatrix}, \quad (5)$$

where a_1 and a_2 are the radii of fiber core and cladding, respectively, $U^2=(k_0^2 n_i^2-\beta^2)a^2$, and $W^2=(\beta^2-k_0^2 n_i^2)a^2$. J_m, N_m, I_m, K_m are the Bessel functions of the first kind, the second kind and the modified Bessel functions of the first kind, the second kind, respectively.

In the fiber cladding layer, the field matrix has the same format as above except that the field elements are written in the function of J_m, N_m, J_m' and N_m' when $kn_2>\beta$ or I_m, K_m, I_m' and K_m' when $kn_2<\beta$.

Based on the continuous boundary conditions, both the propagation constants and the coupling coefficients can be calculated.

In the following numerical simulations, fiber parameters are used as n_1=1.462, n_2=1.457, a_1=4 μm, the LPFG is fabricated with ultraviolet (UV)-induced peak index modulation $\Delta n=1\times10^{-4}$, and grating period is Λ=510 μm.

Firstly, the effect of cladding radius on the effective index is shown in Fig.1. Although the core mode is almost unchanged with the decrease of cladding radius, the radius dependency of the effective index of cladding modes is very obvious, especially the higher-order cladding modes. Since LPFG's resonant wavelength is determined by the difference of effective index according to Eq.(1), the effective index change of cladding modes leads to the resonant wavelength shifting towards much longer wavelength. As can be seen from Fig.2, for the 5th-order cladding mode (ν=5), the resonant wavelength shifts from 1430 nm to 1610 nm when the cladding radius decreases from 62.5 μm to 45 μm. Another feature is that the number of resonant wavelengths is reduced, and only a single resonant wavelength is left in the wavelength range of 1200–1800 nm if cladding radius is less than 20 μm.

To have an overall insight into the LPFG's characteristics of resonant wavelength and transmission depth for different cladding radii, Fig.3 gives LPFG's spectral responses for the cladding radii of 20 μm, 30 μm, 45 μm and 62.5 μm. Obviously, the transmission depth varies and the wavelength shifts with the change of cladding radius. For example, corresponding to the 1st-order cladding mode (ν=1), the depth strengthens from –1 dB to –16 dB when cladding radius decreases from 62.5 μm to 20 μm. It verifies the analyses about the dependency of coupling coefficient on the resonant wavelength and the cladding radius mentioned above.

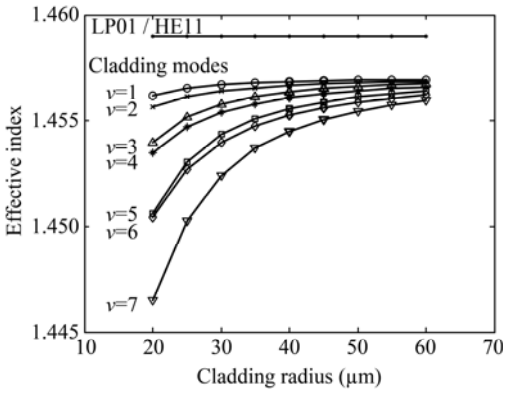

Fig.1 The effect of cladding radius on effective index

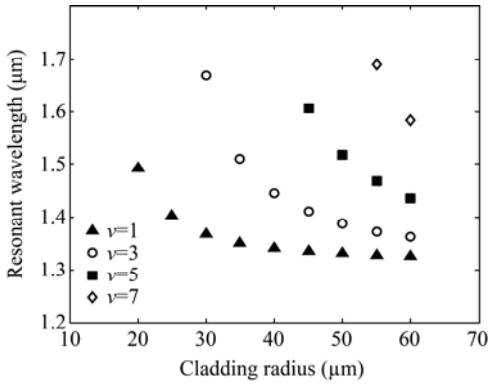

Fig.2 The resonant wavelength versus cladding radius

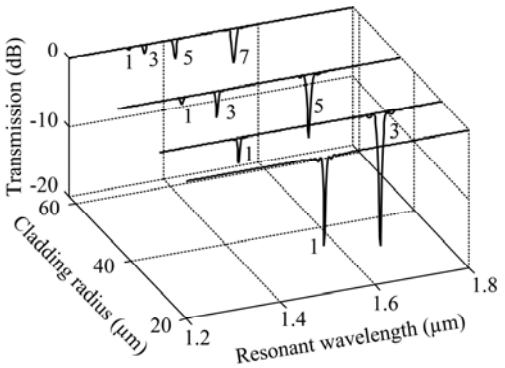

Fig.3 LPFG's spectral responses under four cladding radii

One important application of LPFG is as an external refractive index sensor[11,12]. The external refractive index sensitivities of two LPFGs with cladding radii of 62.5 μm and 45 μm are given in Fig.4(a) and (b), respectively, where the external media are water with refractive index of n_3=1 and alcohol with refractive index of n_3=1.362. We can see that the sensitivity is enhanced with the decrease of cladding radius.

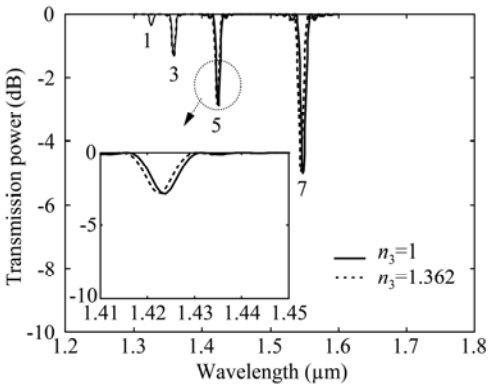

(a) Cladding radius of 62.5 μm

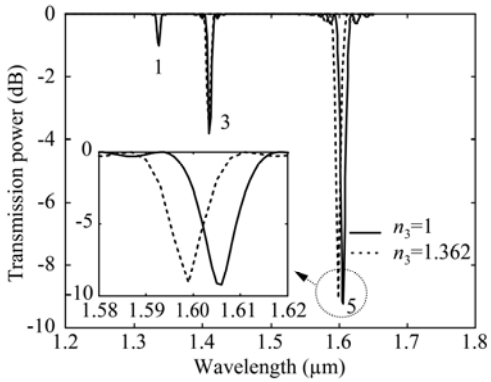

(b) Cladding radius of 45 μm

Fig.4 Influence of cladding radius on the LPFG sensitivity to the external refractive index

Finally, in order to testify the numerical results above, two LPFGs are fabricated in boron and germanium (B-Ge) photosensitive fiber by using 248 nm UV beam with output power of 15 mJ, frequency of 45 Hz and scanning speed of 0.15 mm/s. Both the grating lengths are 50 mm with period of 520 μm. Then, one of them is immersed into hydrogen fluoride (HF) acid for about 20 min so that its cladding radius is reduced to 45 μm. The spectrum characteristics are measured using an LED light source and the optical spectrum analyzer with resolution of 0.1 nm. Fig.5 gives the measured transmission spectra for the 5th-order cladding mode resonance (v=5). Fig.5(a) and (b) show the results for LPFGs without and with HF etching, where the cladding radii are 62.5 μm and 45 μm, respectively. From the comparison, we can see that the central resonance wavelength shifts by about 130 nm towards the longer wavelength and its transmission is deepened. In addition, when LPFG is immersed into different external media (water or alcohol), the wavelength variation is enhanced from about 0.5 nm in LPFG without HF etching to about 5 nm in LPFG with HF etching. Therefore, the sensitivity to external medium is better for LPFG with thinner cladding radius, which is in good agreement with our numerical calculations.

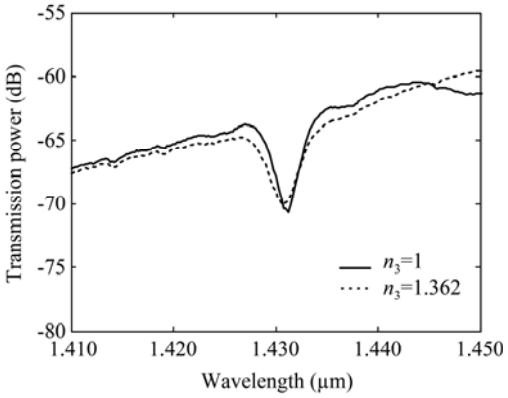

(a) Cladding radius of 62.5 μm

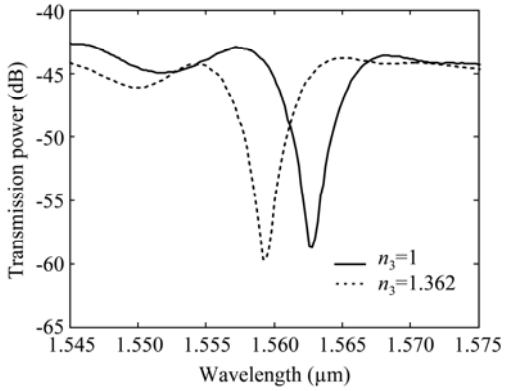

(b) Cladding radius of 45 μm

Fig.5 Experimental results about the influence of cladding radius on the sensitivity of the 5th-order cladding mode in LPFGs

From the numerical analyses and experimental results, we demonstrate that the resonant wavelength and transmission depth can be tuned and the sensitivity to external refractive index can be enhanced significantly by changing the cladding radius of LPFG. Therefore, by choosing proper fiber parameters, LPFG can offer more desirable and feasible characteristics in the chemical sensor.

References

[1] Dong Xiao-wei and Liu Wen-kai, Optoelectronics Letters **8**, 418 (2012).

[2] C. Nidhi, U. Tiwari, N. Panwar, R. S. Kaler, R. Bhatnagar and P. Kapur, IEEE Sensors Journal **13**, 4139 (2013).

[3] Han Ting-Ting, Liu Yan-Ge and Wang Zhi, Journal of Optoelectronics·Laser **23**, 215 (2012). (in Chinese)

[4] Bing Zou and Kin Seng Chiang, Journal of Lightwave Technology **31**, 2223 (2013).

[5] Lei Gao, Tao Zhu, Ming Deng, Kin Seng Chiang, Xiaokang Sun, Xiaopeng Dong and Yusong Hou, IEEE Photonic Journal **4**, 2095 (2012).
[6] T. Allsop and D. J. Webb, Journal of Lightwave Technology **21**, 264 (2003).
[7] Jieliang Li, Weigang Zhang, Shecheng Gao, Pengcheng Geng, Xiaolin Xue, Zhiyong Bai and Hu Liang, IEEE Photonic Technology Letters **25**, 888 (2013).
[8] T. Erdogan, Journal of the Optical Society of America A **14**, 1760 (1997).
[9] Kaiming Zhou, Haitao Liu and Xiongwei Hu, Optics Communications **197**, 295 (2001).
[10] Allan W. Snyder and John D. Love, Optical Waveguide Theory, New York: Chapman and Hall, 1983.
[11] Heather J. Patrick, Alan D. Kersey and Frank Bucholtz, Journal of Lightwave Technology **16**, 1606 (1998).
[12] Shi Sheng-Hui, Zhou Xiao-Jun, Zhang Zhi-Yao and Liu Yong, Journal of Optoelectronics·Laser **23**, 1644 (2012). (in Chinese)